



## OPEN Inter-and intra-period dietary variations revealed by dental microwear texture analysis in Holocene Levantine populations

Dana Megreli<sup>1,4</sup>, Ariel Pokhojaev<sup>1,4</sup>, Hila May<sup>2,3</sup>, Daniel Zvi Bar<sup>1</sup> & Rachel Sarig<sup>1,3</sup>✉

The transition from hunter-gatherer subsistence to agricultural economies marks one of the most significant shifts in human dietary history. This study investigates dietary adaptations and intra-period variability among Holocene Levantine populations using dental microwear texture analysis (DMTA). Combining Scale-Sensitive Fractal Analysis (SSFA) with 3D surface texture (3DST) standards, we analyzed second molar occlusal facets from 78 individuals across Natufian, Pre-Pottery Neolithic (PPN), Chalcolithic, and modern Bedouin groups. Our results demonstrate clear inter-period dietary transitions, with Natufian hunter-gatherers exhibiting smoother enamel surfaces with high anisotropy, indicative of a diet reliant on minimally processed resources. In contrast, subsequent PPN and Chalcolithic populations showed progressively increased complexity, deeper pits, and reduced anisotropy, reflecting the incorporation of abrasive foods associated with advanced cereal processing techniques and stone grinding tool usage. Principal Component Analysis revealed distinct clustering by chronological periods and highlighted intra-period variability driven by localized subsistence strategies and food processing practices. Within the PPN, significant microwear differences emerged between PPNC and PPNB sub-periods, suggesting nuanced dietary shifts potentially related to changing resource availability or food preparation methods. Chalcolithic populations demonstrated further dietary diversification, underscoring regional variations in subsistence practices. Our findings emphasize the value of integrating SSFA and 3DST methodologies for capturing subtle dietary distinctions, thereby enhancing our understanding of ancient dietary adaptations and technological innovations during the pivotal Neolithic transition.

**Keywords** Dental microwear texture analysis (DMTA), Neolithic transition, Dietary reconstruction, Levantine populations, Food processing techniques

The evolutionary history of hominins in the Levant is marked by significant shifts in economic behaviors, subsistence strategies, and dietary patterns. One of the most transformative processes in human history, known as the Neolithization process, represents the transition from a subsistence-based food gathering and hunting to a food-producing society, agriculture, animal domestication, and permanent settlement (14,900–8,250 cal BP)<sup>1–4</sup>.

This transformation began with the Natufian population (14,900–11,750 cal BP), who were part of the terminal hunter-gatherer societies of the Pleistocene in the southern Levant. The Natufians were either nomadic or semi-sedentary, living in small groups<sup>5–7</sup>. Their subsistence strategies relied on hunting, which required extensive physical exertion and large hunting territories<sup>8–11</sup>. In addition to hunting, they engaged in wild cereal harvesting, food processing (e.g., pounding), and small-scale construction activities such as the construction of rounded low-walled structures<sup>7,12–15</sup>.

Following the Natufians, the Pre-Pottery Neolithic A (PPNA) population (~12,175–10,500 cal BP) introduced small-scale cultivation and hunting of smaller animals<sup>16–18</sup>. Their construction activity was limited and consisted of freestanding or semi-subterranean rounded structures, built on low walls with minimal floors<sup>1,4,10,19,20</sup>. This period was succeeded by the Pre-Pottery Neolithic B (PPNB) (~10,500–8,700 cal BP), during which food

<sup>1</sup>Department of Oral Biology, the Maurice and Gabriela Goldschleger School of Dental Medicine, Gray Faculty of Medical & Health Sciences, Tel Aviv University, 6997801 Tel Aviv, Israel. <sup>2</sup>Department of Anatomy and Anthropology, Gray Faculty of Medical & Health Sciences, Tel Aviv University, 6997801 Tel Aviv, Israel. <sup>3</sup>Dan David Center for Human Evolution and Biohistory Research, Gray Faculty of Medical & Health Sciences, Tel Aviv University, 6997801 Tel Aviv, Israel. <sup>4</sup>Dana Megreli and Ariel Pokhojaev contributed equally to this project. ✉email: sarigrac@tauex.tau.ac.il

production became more complex and widespread, accompanied by the domestication of plants and animals. The PPNB period also marked a shift to a more sedentary lifestyle<sup>7,16,21–24</sup>. The PPNB people built more durable homes from stone and mud bricks, with floors often covered in plaster<sup>1,25–28</sup>. They participated in various activities, including tilling, harvesting, seed-grinding, mud-brick production, lime plaster formation, and land clearing<sup>1,2,4,25,29</sup>. The Pre-Pottery Neolithic C (PPNC) (~8,600–8,250 cal BP) shared many characteristics with the earlier PPNB but expanded to include bovine domestication<sup>18</sup> and introduced new occupations such as fishing and seafaring<sup>30,31</sup>.

Following the Pre-Pottery Neolithic, the Chalcolithic period (~6,500–5,500 cal BP), also known as the Copper Age, emerged as a transitional phase into the Bronze Age. During this time, agriculture intensified, with increased cultivation of cereals and a growing reliance on fruits like olives, as well as the use of animal secondary products such as wool and dairy<sup>32,33</sup>. Technological advancements in ceramics, stonework, and ivory carving further distinguished this era<sup>34</sup>.

These major changes during the terminal Pleistocene had a tremendous impact on the population's diet, health, demographics, mobility, and physical stress patterns<sup>2,9,35–37</sup>.

Beyond oral pathologies and mandible size, occlusal dental wear can provide additional clues about dietary habits<sup>38–42</sup>. Analyzing dental wear patterns on macroscopic and microscopic scales indicates the abrasiveness of the food and the dental function<sup>41,43,44</sup>.

Dental microwear texture analysis (DMTA) is one of the most commonly employed approaches for reconstructing diets and subsistence strategies in extinct species and past human populations<sup>42,45–48</sup>. While both occlusal and buccal surfaces preserve microwear textures<sup>49</sup>, buccal textures are more affected by exogenous abrasives and food-processing<sup>50</sup>. To limit cultural/behavioural confounds, in the present study we analyzed occlusal facet 9, which predominantly reflects dietary signals. Facet 9 is located on the mesiolingual cusp of maxillary molars (Fig. 1A) or the distobuccal cusp of mandibular molars (Fig. 1B). This facet develops during Phase II of the chewing cycle and is subjected to both compressive and shear forces, making it a standard and reliable surface for dental microwear texture analysis (DMTA)<sup>51–53</sup>. DMTA employs analyzing microscopic features on dental enamel using a visible-light scanning confocal measuring system to obtain three-dimensional coordinate matrices and generate digital models of the scanned surfaces (Fig. 1C–H)<sup>54</sup>. These models are analyzed to quantify and mathematically characterize the dental microwear texture. Scale-Sensitive Fractal Analysis (SSFA) provides a quantitative framework for characterizing surface textures, implemented via SFRax and Toothfrax software (Surfract, [www.surfract.com](http://www.surfract.com)), originally developed for precision surface metrology. Ungar et al.<sup>55</sup> pioneered the application of SSFA in combination with confocal microscopy for the analysis of dental microwear textures, which has since become an established method for reconstructing dietary habits in archaeological and paleontological contexts<sup>55</sup>. SSFA studies commonly emphasize two key variables that effectively differentiate dietary strategies: area-scale fractal complexity (*Asfc*) and exact proportion length-scale anisotropy of relief [*epLsar* (1.8)]<sup>53,55–57</sup>.

In parallel, a complementary approach employs three-dimensional areal surface texture parameters derived from engineering standards, specifically ISO 25178-2 (International Organization for Standardization<sup>58</sup>). Schulz et al.<sup>44</sup> demonstrated the applicability of these standardized parameters for dietary reconstruction and the identification of dietary traits in fossil hominin populations<sup>44</sup>. ISO 25178-2 defines 30 roughness parameters, categorized into six groups that describe distinct aspects of surface texture: height, functional (plane), spatial, hybrid, functional (volume), and feature parameters (Table 1). The aim of the study is to provide new information on the variation in food preparation techniques of archaic Levantine populations during the Neolithization process through dental microwear analysis. By utilizing both SSFA and 3DST methods to study wear patterns, we aim to reveal the subtle variations in microwear patterns between and within each period.

## Results

### Inter periods comparison

#### Scale-sensitive fractal analysis (SSFA)

The Kolmogorov-Smirnov test for normality demonstrated that complexity (*Asfc*) followed a normal distribution ( $p = 0.2$ ), whereas anisotropy (*epLsar*) exhibited a non-normal distribution ( $p = 0.017$ ). Thus, a one-way ANOVA was performed to compare the effect of periods on complexity, and the Kruskal-Wallis test was performed to compare the effect of periods on anisotropy.

The one-way ANOVA revealed a statistically significant difference in the complexity between the groups ( $p = 0.003$ ). Post hoc analysis using Tukey's HSD test for multiple comparisons indicated that the Natufian group (mean = 1.635, SD = 0.815) exhibited significantly lower complexity (*Asfc*) values compared to the Chalcolithic (mean = 2.59, SD = 0.725) and Modern groups (mean = 2.349, SD = 0.688;  $p = 0.026$ ) (Fig. 3A). A non-significant trend indicated higher complexity values in the Pre-Pottery Neolithic group (mean = 2.262, SD = 0.805) compared to the Natufian group ( $p = 0.054$ ). No statistically significant differences were found between the other groups (Fig. 3A, Table 1).

The Kruskal-Wallis test indicated a statistically significant difference in anisotropy between at least two groups ( $\chi^2[3]=15.116$ ;  $p = 0.002$ ). Subsequent Bonferroni correction for multiple comparisons revealed that the Natufian group had significantly higher anisotropy (mean = 0.0042, SD = 0.0015) compared to the Chalcolithic group (mean = 0.003, SD = 0.001;  $p = 0.043$ ) and the Modern group (mean = 0.0026, SD = 0.0006;  $p = 0.001$ ) (Fig. 3B). No significant differences were found between the other groups ( $p > 0.05$ ) (Fig. 3B, Table 1).

#### 3D areal surface texture standards (ISO/DIS 25178)

Surface texture parameters from ISO 25178-2 were analyzed for normality using the Kolmogorov-Smirnov test. Normally distributed variables were analyzed using one-way ANOVA, while non-normally distributed variables were analyzed using the Kruskal-Wallis test. A total of 24 out of 30 parameters exhibited significant differences

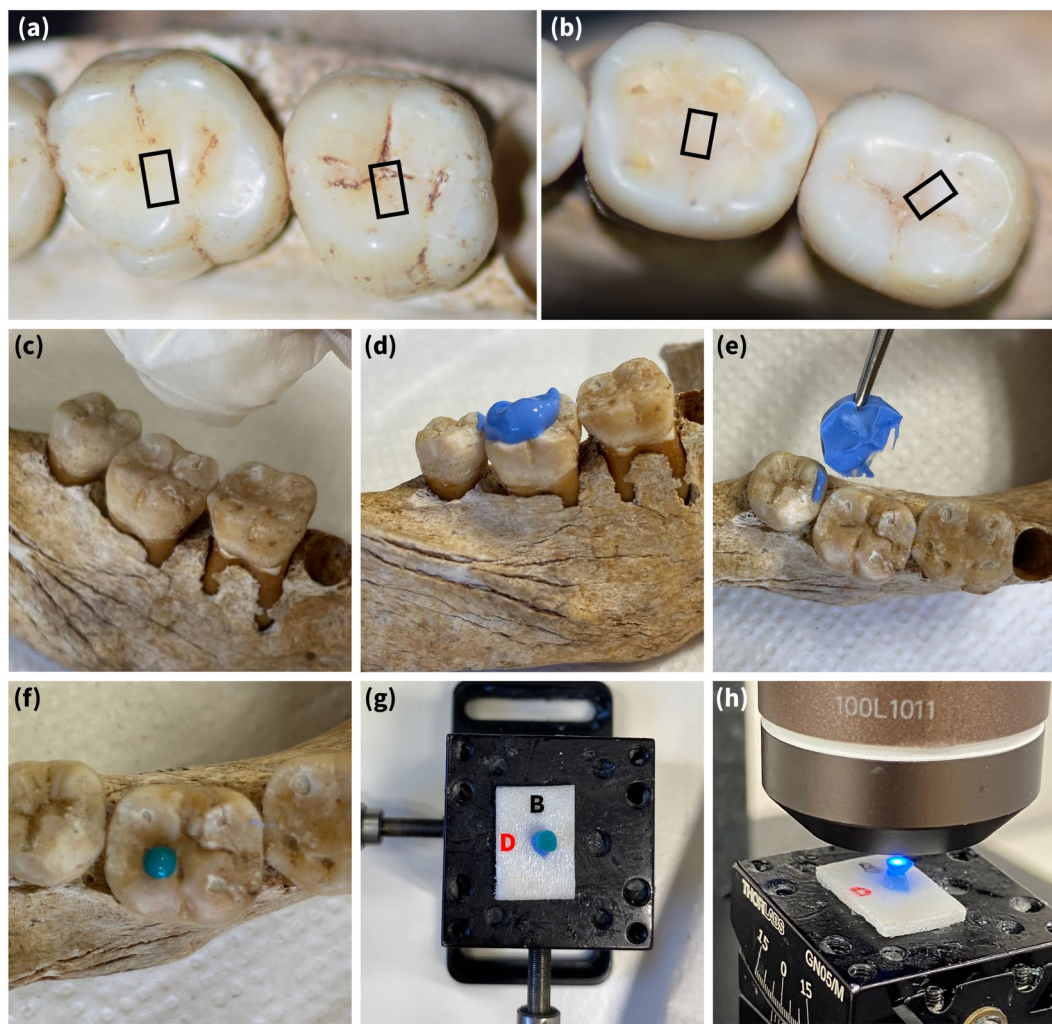


**Fig. 1.** Location of facet 9 (rectangular area) on molars from a Chalcolithic individual (Peqi'in, Israel): **(a)** Left maxillary molars; **(b)** Right mandibular molars; and DMTA workflow: **(c)** Removal of contaminants using cotton wool; **(d)** impression taking; **(e)** complete polymerization of impression material followed by careful removal; **(f)** targeted molding of facet 9; **(g)** orientation tracking via buccal and distal reference marks; and **(h)** surface scanning.

between the four study populations. Post-hoc analyses with correction for multiple comparisons were performed for significant variables (Table 1).

#### Principal component analysis (PCA)

To elucidate differences in dental microwear textures among prehistoric Levantine populations and evaluate the combined impact of parameters from scale-sensitive fractal analysis (SSFA) and ISO/DIS 25178-2 analyses, we employed Principal Component Analysis (PCA). Our aim was to evaluate the multivariate signal of 3DST together with DMTA rather than rely on any single metric. As shown in Table 1, 24 of 30 3DST parameters exhibit statistically significant differences in at least one pairwise comparison among the four populations. From the 24 parameters that showed statistical significance, we retained the two most informative dietary signature parameters from each significant parameter group (10 parameters in total) for PCA to avoid redundancy and preserve interpretability. The selected set represents the ISO 25178 parameter families (height:  $Sa$ ,  $Sv$ ; functional [plane]:  $Smr$ ,  $Sxp$ ; hybrid:  $Sdr$ ,  $Sdq$ ; functional [volume]:  $Vm$ ,  $Vv$ ; feature:  $Spd$ ,  $Shv$ ) (Fig. 3C). Spatial group parameters were found to be non-significant. Segregation in the PCA was driven by geographic regions and sub-periods rather than solely by chronological periods.

The resulting plot (Fig. 3C) reveals separation between the Natufian and Chalcolithic populations along the PC1 axis, which accounts for 51.5% of the total variance, with minor overlap involving Peqi'in individuals. The Natufian group is also distinguished from the Pre-Pottery Neolithic population along PC1, showing minimal overlap with the Pre-Pottery Neolithic B (PPNB) sub-period. In contrast, the Chalcolithic population shows separation from the PPNC sub-period along the PC2 axis, representing 19.2% of the total variance. Modern specimens displayed considerable variation across all parameters, overlapping with all four prehistoric groups,

Surface texture parameter	Units	Natufian (n=19)		Pre-Pottery Neolithic (n=21)		Chalcolithic (n=19)		Modern (n=19)		Sig.	Post Hoc
		Mean	SD	Mean	SD	Mean	SD	Mean	SD		
Complexity (Asfc) <sup>b</sup>	unitless	1.635	0.8154	2.262	0.8048	2.59	0.7248	2.349	0.6884	0.003	Nat ≠ Chal, Mod
Anisotropy (epLsar) <sup>b</sup>	unitless	0.0042	0.0015	0.0033	0.0012	0.003	0.001	0.0026	0.0006	0.002	Nat ≠ Chal, Mod
Scale of maximum complexity (Smfc) <sup>b</sup>	unitless	1.026	0.08	1.466	0.119	1.065	0.359	1.197	0.062	0.003	Nat ≠ Neo
Heterogeneity of Asfc (HAsfc) <sup>b</sup>	unitless	0.314	0.046	0.428	0.04	0.278	0.201	0.2946	0.02	0.007	Neo ≠ Chal, Mod
Height											
Root-mean-square height (Sq) <sup>b</sup>	μm	0.372	0.106	0.700	0.237	0.582	0.135	0.589	0.165	0.001	Nat ≠ Neo, Chal, Mod
Skewness (Ssk) <sup>a</sup>	unitless	-0.709	0.394	-0.543	0.366	-0.528	0.464	-0.680	0.386	NS	
Kurtosis (Sku) <sup>b</sup>	unitless	5.250	1.582	4.304	0.897	4.883	1.724	4.141	0.737	NS	
Maximum peak height (Sp) <sup>a</sup>	μm	1.337	0.358	2.425	0.946	2.113	0.621	1.866	0.543	0.001	Nat ≠ Neo, Chal
Maximum pit height (Sv) <sup>a</sup>	μm	2.123	0.682	3.189	0.716	2.837	0.683	3.024	0.689	0.001	Nat ≠ Neo, Chal, Mod
Maximum height (Sz) <sup>a</sup>	μm	3.453	0.929	5.846	1.789	5.057	1.000	4.946	1.208	0.001	Nat ≠ Neo, Chal, Mod
Arithmetic mean height (Sa) <sup>b</sup>	μm	0.280	0.082	0.539	0.190	0.443	0.113	0.459	0.135	0.001	Nat ≠ Neo, Chal, Mod
Functional (plane)											
Areal material ratio (Smr) <sup>b</sup>	%	35.662	24.471	2.464	2.063	4.669	5.155	8.154	4.790	0.001	Nat ≠ Neo, Chal; Neo ≠ Mod
Inverse areal material ratio (Smc) <sup>a</sup>	μm	0.419	0.119	0.761	0.248	0.669	0.192	0.684	0.203	0.001	Nat ≠ Neo, Chal, Mod
Extreme peak height (Sxp) <sup>a</sup>	μm	0.883	0.295	1.599	0.447	1.281	0.246	1.368	0.371	0.001	Nat ≠ Neo, Chal, Mod; Neo ≠ Chal
Spatial											
Autocorrelation length (Sal) <sup>a</sup>	μm	13.511	2.557	14.849	2.616	14.655	2.261	15.354	2.137	NS	
Texture-aspect ratio (Str) <sup>a</sup>		0.540	0.146	0.566	0.101	0.639	0.136	0.620	0.123	NS	
Texture direction (Std) <sup>a</sup>	°	109.259	33.677	110.111	23.683	108.007	27.301	108.811	26.720	NS	
Hybrid											
Root mean-square gradient (Sdq) <sup>a</sup>		0.149	0.036	0.187	0.032	0.192	0.028	0.185	0.028	0.001	Nat ≠ Neo, Chal, Mod
Developed interfacial area ratio (Sdr) <sup>a</sup>	%	1.134	0.481	1.783	0.563	1.836	0.506	1.711	0.513	0.001	Nat ≠ Neo, Chal, Mod
Functional (volume)											
Material volume (Vm) <sup>a</sup>	μm <sup>3</sup> /μm <sup>2</sup>	0.014	0.003	0.029	0.011	0.025	0.005	0.022	0.006	0.001	Nat ≠ Neo, Chal, Mod; Neo ≠ Mod
Void volume (Vv) <sup>a</sup>	μm <sup>3</sup> /μm <sup>2</sup>	0.434	0.122	0.838	0.306	0.695	0.194	0.706	0.208	0.001	Nat ≠ Neo, Chal, Mod
Peak material volume (Vmp) <sup>a</sup>	μm <sup>3</sup> /μm <sup>2</sup>	0.014	0.003	0.029	0.011	0.025	0.005	0.022	0.006	0.001	Nat ≠ Neo, Chal, Mod; Neo ≠ Mod
Core material volume (Vmc) <sup>a</sup>	μm <sup>3</sup> /μm <sup>2</sup>	0.306	0.091	0.598	0.226	0.497	0.145	0.519	0.163	0.001	Nat ≠ Neo, Chal, Mod
Core void volume (Vvc) <sup>a</sup>	μm <sup>3</sup> /μm <sup>2</sup>	0.378	0.105	0.693	0.237	0.611	0.177	0.623	0.192	0.001	Nat ≠ Neo, Chal, Mod
Pit void volume (Vvv) <sup>a</sup>	μm <sup>3</sup> /μm <sup>2</sup>	0.056	0.019	0.098	0.025	0.079	0.015	0.083	0.022	0.001	Nat ≠ Neo, Chal, Mod; Neo ≠ Chal
Feature											
Density of peaks (Spd) <sup>b</sup>	1/μm <sup>2</sup>	0.004	0.002	0.002	0.001	0.003	0.001	0.002	0.001	0.001	Neo ≠ Nat, Chal
Arithmetic mean peak curvature (Spc) <sup>a</sup>	1/μm <sup>2</sup>	0.622	0.173	0.642	0.180	0.763	0.210	0.699	0.188	NS	
Ten-point height (S10z) <sup>b</sup>	μm	2.777	0.746	4.532	1.150	4.123	0.640	3.982	0.920	0.001	Nat ≠ Neo, Chal, Mod
Five-point peak height (S5p) <sup>a</sup>	μm	1.082	0.276	1.878	0.616	1.717	0.413	1.532	0.351	0.001	Nat ≠ Neo, Chal, Mod
Five-point pit height (S5v) <sup>a</sup>	μm	1.695	0.537	2.654	0.581	2.376	0.497	2.450	0.659	0.001	Nat ≠ Neo, Chal, Mod
Mean dale area (Sda) <sup>a</sup>	μm <sup>2</sup>	232.675	91.461	483.885	235.978	388.542	133.863	384.179	145.130	0.001	Nat ≠ Neo, Chal, Mod
Mean hill area (Sha) <sup>b</sup>	μm <sup>2</sup>	256.209	105.474	493.625	231.184	296.477	97.049	402.472	170.668	0.001	Nat ≠ Neo, Mod; Neo ≠ Chal
Mean dale volume (Sdv) <sup>a</sup>	μm <sup>3</sup>	2.959	1.477	8.508	3.788	7.494	4.007	7.622	3.613	0.001	Nat ≠ Neo, Chal, Mod
Mean hill volume (Shv) <sup>b</sup>	μm <sup>3</sup>	4.125	2.897	14.373	9.411	7.735	4.129	11.077	5.817	0.001	Nat ≠ Neo, Mod

**Table 1.** Descriptive statistics for surface texture parameters (ISO 25178-2) between the four periods. Nat, Natufian; Neo, Pre-Pottery Neolithic; Chal, Chalcolithic; Mod, Modern. <sup>a</sup>One-way analysis of variance with post hoc analysis (Tukey). <sup>b</sup>Kruskal-Wallis with post hoc analysis (Bonferroni)

as expected. The Natufian sites of Hayonim and Eynan-Malha exhibit complete overlap along PC1, with PC2 likewise failing to differentiate between them.

Regarding Pre-Pottery Neolithic sub-periods (PPNB and PPNC), a notable separation emerges along PC2. Overview of the 14 parameters yields the following observations (Fig. 3C) :

- **Natufian:** Higher values for *Smr* and *epLsar*, with relatively lower values for *Asfc*, *Sdr*, and *Sdq*.
- **Pre-Pottery Neolithic B :** Higher *Spd*, *Sdq*, *Sdr*, and *Asfc*, with lower *Smr*, *epLsar*, *Hasfc*, and *Smfc*.
- **Pre-Pottery Neolithic C :** Higher *Shv*, *Vm*, *Sa*, *Vv*, *Sxp*, *Hasfc*, and *Smfc*, with lower *Spd* and *Smr*.
- **Chalcolithic:** Higher *Spc*, *Sdq*, *Sdr*, and *Asfc*, with lower values for *Smr* and *epLsar*.
- **Modern:** Broad variability across parameters, overlapping with all other groups.

### Intra-period comparison: pre-pottery neolithic B and pre-pottery neolithic C

#### Scale-sensitive fractal analysis (SSFA)

The Pre-Pottery Neolithic B (PPNB) and Pre-Pottery Neolithic C (PPNC) SSFA results underwent a Kolmogorov-Smirnov test for normality, and demonstrated a normal distribution both for complexity ( $p = 0.2$ ) and anisotropy ( $p = 0.2$ ). Thus, a T-test with Levene's Test for Equality of Variances was performed to compare the effect of the sub-periods on complexity and anisotropy. A T-test revealed that there was not a statistically significant difference in anisotropy (*epLsar*) between the PPNB (mean = 0.003, SD = 0.002) and PPNC (mean = 0.0035, SD = 0.001) groups. However, there was a statistically significant difference ( $p = 0.027$ ) in the complexity (*Asfc*) between the two groups: PPNB (mean = 3.101, SD = 0.944) versus PPNC (mean = 1.926, SD = 0.43).

#### 3D areal surface texture standards (ISO/DIS 25178)

With the exception of a singular value (*Sdq*), our statistical analysis yielded no significant differences between the groups. Subtle differences in surface patterns can be discerned between the two groups. Individual representing the PPNC group, shows a dental microwear pattern characterized by fewer pits and shallower scratches when compared to the specimen that comes from the PPNB group and exhibits a noticeably greater number of pits and deeper scratches. However, aside from this distinction, the surface characteristics between the two individuals appear to be quite similar (Fig. 2).

#### Principal component analysis (PCA)

To test whether dental microwear textures could discriminate between the Pre-Pottery Neolithic B (PPNB) and Pre-Pottery Neolithic C (PPNC) sub-periods, a targeted PCA was performed on two representative ISO parameters (material ratio, *Smr*, and peak density, *Spd*) together with three SSFA variables - surface complexity (*Asfc*), scale of maximum complexity (*Smfc*), and heterogeneity of complexity (*Hasfc*). The first two principal components accounted for 67.8% of the total variance (PC1=44.2%; PC2=23.6%) (Fig. 3D).

PC1 captured the chronological contrast. PPNC teeth plotted predominantly on the negative side of PC1 and were characterised by markedly higher *Hasfc* values, indicating more heterogeneous surface complexity (Fig. 3D). In contrast, PPNB assemblages (Abu Gosh and Kfar HaHoresh) loaded positively on PC1 and exhibited greater *Spd* and *Asfc*, reflecting a higher density of small peaks and overall surface complexity (Fig. 3D). PC2 resolved intra-period, site-specific variation. PPNC Atlit-Yam and PPNB Abu Gosh grouped together on the positive end of PC2, distinguished by elevated *Smr* (a larger proportion of plateau-like areas) and reduced *Smfc* (finer scales of maximum complexity). Conversely, PPNC Motza and PPNB Kfar HaHoresh plotted on the negative PC2 axis, showing the reverse pattern (higher *Smfc* and lower *Smr*) suggesting coarser textural scales with fewer plateau surfaces.

### Intra-period comparison: chalcolithic sites

#### Principal component analysis (PCA)

Due to small sample size of the sub-groups, no statistical tests were performed. A separate Principal Component Analysis (PCA) was conducted for Chalcolithic sites using three significant ISO parameters (*Smr*, *Sa*, *Spd*) and three SSFA variables (*Asfc*, *Smfc*, *Hasfc*). Together, PC1 and PC2 accounted for 93.4% of total variance, clearly distinguishing between the sites (Fig. 3E). PC1 exhibited strong positive loadings for peak-related metrics (*Spd*, *Smr*, *Asfc*) and strong negative loading for textural heterogeneity (*Hasfc*), contrasting densely peaked and homogeneous textures against more heterogeneous surfaces. PC2 differentiated surface amplitude and scale through positive loadings for mean surface height (*Sa*) and scale of maximum complexity (*Smfc*).

Microwear patterns observed from the analysis of the six parameters are summarized as follows:

- **Motza (n=1)** positioned at the extreme positive end of PC1 and near the origin of PC2, characterized by high *Asfc*, *Smr* and *Spd* values with low *Hasfc*.
- **Safsuf (n=3)** occupied the extreme positive end of PC2, indicating high *Sa* and *Smfc* values.
- **Asawir (n=2)** presented with highest *Smfc* and *Hasfc*.
- **Nahal Soreq (n=1)** appeared low on PC2 and slightly negative on PC1, displaying the lowest *Sa* and relatively low *Smfc* and *Smr*.
- **Peqi'in (n=12)** clustered centrally near the origin, exhibiting intermediate values across parameters.

### Discussion

The application of dental microwear texture analysis has advanced our ability to reconstruct past human diets. In this study, by integrating SSFA with ISO-compliant 3DST, we aimed not only to trace the established diachronic dietary trends from Natufian hunter-gatherers to Chalcolithic agriculturalists but also to uncover previously underexplored patterns of intra-period variability. This dual-metric framework was chosen to expose the

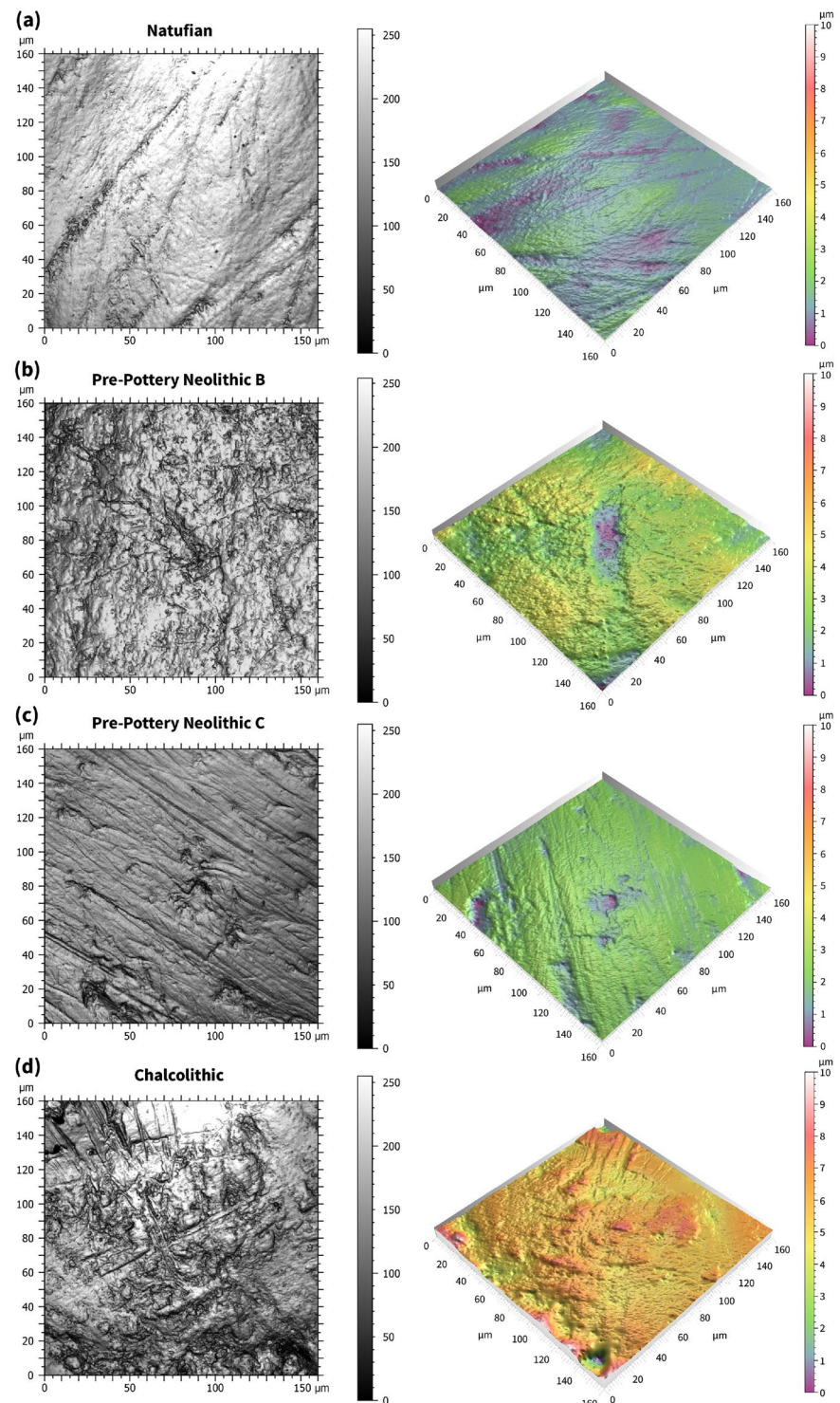


**Fig. 2.** Surface texture analysis of facet 9 on mandibular second molars. **Left:**  $160 \times 160 \mu\text{m}$  image of the facet impression; **Right:** Reconstructed 3D topographic view. Distinct surface texture patterns are evident between (a) Natufian, (b) Pre-Pottery Neolithic B (PPNB), (c) Pre-Pottery Neolithic C (PPNC), and (d) Chalcolithic wear facets.

subtler, intra-period grain of dietary variation (if present) that is often obscured when SSFA or 3DST are used in isolation<sup>44,59</sup>. Our results demonstrate that beyond the broad inter-period dietary transitions often emphasized in macroevolutionary models, there exists a some degree of heterogeneity within periods - suggesting diverse subsistence strategies, ecological adaptations, and potentially localized cultural practices.

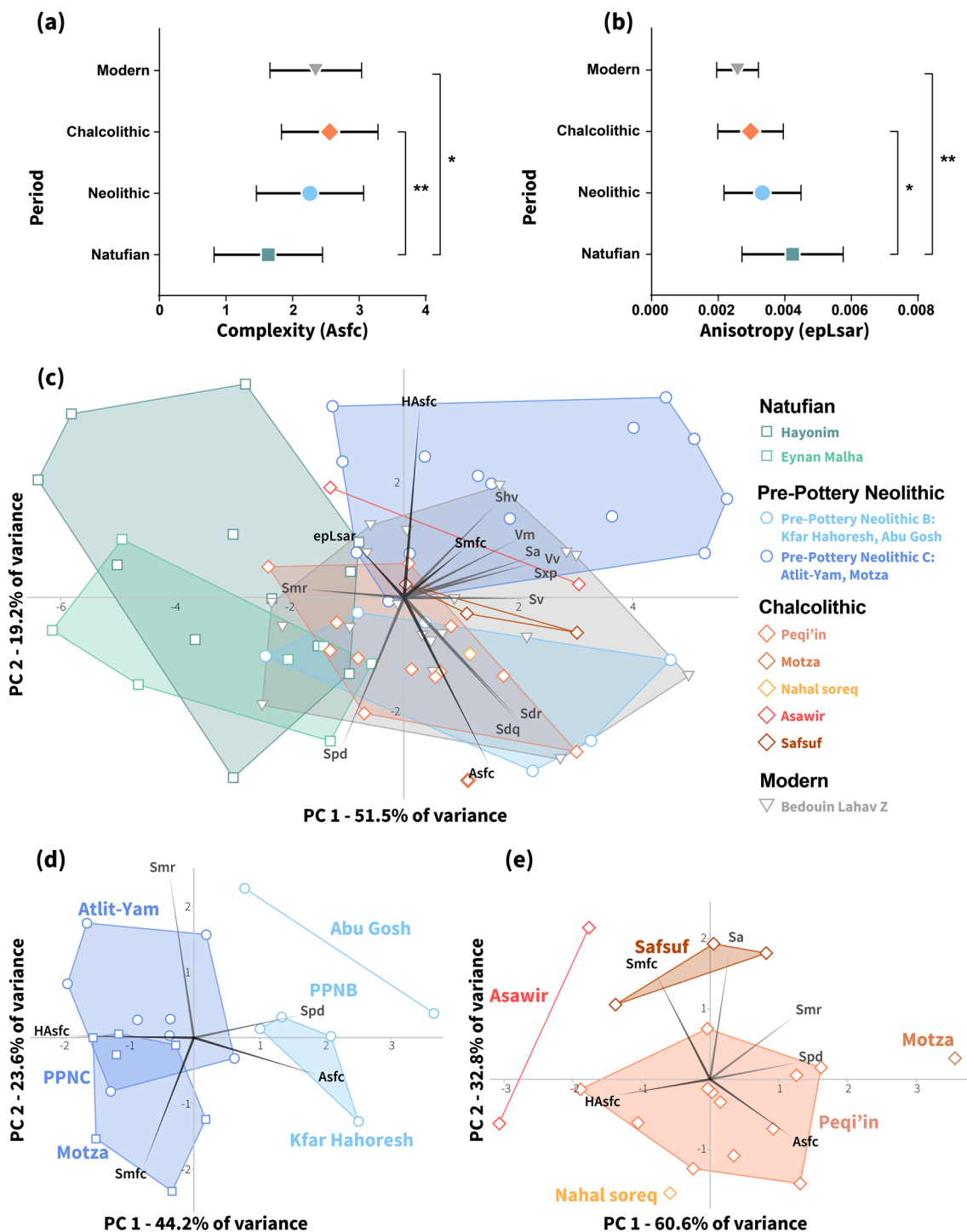


**Fig. 3.** Graphical representation of the study results. See Table 1 for definitions of all abbreviated parameters. **Top:** Comparison of (a) complexity (Asfc), and (b) anisotropy (epLsar) between the four periods. **Middle:** (c) Principal Component Analysis (PCA) of dental microwear parameters from Scale-Sensitive Fractal Analysis (SSFA) and ISO/DIS 25178-2 standards. Grouped and color-coded based on geographic regions and sub-periods. Vectors represent individual parameters, illustrating their contributions to group differentiation. **Bottom:** (d) PCA of the Asfc, Hasfc, Smfc, Smr, and Spd parameters visualizing the PPNC and PPNB sub-periods. (e) PCA of Asfc, Hasfc, Smfc, Sa, Smr, and Spd parameters across multiple Chalcolithic sites.

In the inter-period PCA on the 14 combined 3DST and SSFA variables, the combined methods distinctly characterized the Natufian group with relatively low surface complexity (Asfc) and high anisotropy (epLsar) (Fig. 3C). PC1 primarily distinguishes samples by overall surface roughness and complexity versus anisotropy. High positive PC1 scores correspond to teeth with rough, complex surfaces (high Sa, Sv, Sdr, Asfc) and low epLsar -

characteristic of the farming groups. Negative PC1 scores align with smoother, directional scratch-dominated surfaces (lower surface complexity ( $Asfc$ ), high anisotropy ( $epLsar$ )) (Fig. 3C).

The Natufian dietary signal (relatively high  $epLsar$ , low  $Asfc$ ) as consistent with more directional chewing and less exogenous grit, whereas the farmer groups' higher  $Asfc$  and lower  $epLsar$  may reflect greater exposure to abrasives introduced by intensified processing (grinding/milling). Archaeological records report rising grindstone frequencies through the later Upper Paleolithic into the Neolithic, with deeply concave working faces (markers of heavier, repeated use) becoming common only after the Natufian period<sup>60</sup>. Accordingly, the higher complexity in early farmers is better interpreted as a signature of processing intensity, not broader consumption of unprocessed wild foods. These results accord with Schmidt et al.<sup>42</sup>, who likewise found no significant SSFA differences for largely overlapping sites. Compared to previous studies<sup>42,60,61</sup>, minor discrepancies in absolute values measured could be attributed to slightly different sites and sample size, as well as minor methodological differences. The inference remains unchanged - no significant difference between these groups in  $Asfc$  or  $epLsar$ .

This interpretation aligns the reduced height (e.g.,  $Sq$ ,  $Sa$ ) and volume-related surface parameters ( $Vm$ ,  $Vv$ ) observed in Natufians with the archaeological evidence supporting a preagricultural forager lifestyle<sup>19</sup> reliant on wild plant resources and less processed meat consumption<sup>19,62,63</sup>, typically requiring directional chewing movements rather than grinding actions.

Natufian sites of Hayonim and Eynan Malha exhibit low PC1 scores (reflecting their smoother, less pitted surfaces and high anisotropy), while early farmers cluster on the opposite end with high PC1 (rough, pitted surfaces with low anisotropy) (Fig. 3C).

Conversely, subsequent populations (Pre-Pottery Neolithic, Chalcolithic, Modern) exhibited higher complexity, hybrid, and feature parameters, indicative of diets enriched with harder and more abrasive food, likely linked to the widespread adoption of cereal grains and stone grinding tools, consistent with archaeological and botanical evidence from these periods<sup>64–66</sup>. The modern Bedouin specimens plot in an overlap with the PPN and Chalcolithic clusters, suggesting that the modern group has a high variability in the microwear texture pattern. The clear separation between the preagricultural hunter gatherers with farming societies along the dominant PC1 confirms the strong influence of subsistence change on microwear: the transition from foraging to farming corresponds to a major shift in overall texture profile (Fig. 3C). PC2 appears to capture more subtle differences, including variation in the frequency of microscopic peaks vs. valleys and heterogeneity, indicating variability within agricultural diets available at various sites, or perhaps differences between early and later farmers, but the Natufian vs. farmer distinction remains the clearest pattern in the data (Fig. 3C). For instance, PPNB and PPNC samples differ slightly along PC2: PPNB teeth tend to have slightly more numerous micro-peaks and more homogeneous texture (lower  $Hasfc$ ), plotting with the Chalcolithic sample on the negative extreme of PC2, whereas PPNC show lower fractal complexity ( $Asfc$ ) and higher heterogeneity ( $Hasfc$ ) (Fig. 3C).

Significantly higher ( $Asfc$ ) values in the PPNB group ( $p = 0.027$ ) may reflect a diet that included a greater variety of processed foods, while the lower ( $Asfc$ ) in the PPNC group could indicate a shift towards simpler dietary practices and limited agricultural productivity, possibly due to changes in subsistence strategies and environmental pressures<sup>7,18</sup>.

Higher values of parameters such as root-mean-square height ( $Sq$ ), arithmetic mean height ( $Sa$ ), peak density ( $Spd$ ), complexity, and pit size (as indicated by volume and feature parameters) suggest that the diet became harder during the Pre-Pottery Neolithic period and continued this trend into the Chalcolithic (Table 1). These findings likely reflect a greater reliance on agricultural products and more intensive food processing techniques, such as grinding and milling with stone tools<sup>64</sup>. These tools used by these early agriculturalists, made of sandstone, limestone, and basalt, contained hard grit particles like quartz, which are tougher than enamel<sup>65,66</sup>. Frequent use of these grinding tools may have introduced significant amounts of abrasive particles into the diet, contributing to the development of a harder diet and resulting in larger pits on dental surfaces, as previously suggested by Pastor<sup>67</sup>.

Differences in areal material ratio ( $Smr$ ) and inverse areal material ratio ( $Smc$ ) across periods further support the transition from hunter-gatherer to agricultural economies (Fig. 3C, Table 1). The Natufian group's higher  $Smr$  and lower  $Smc$  reflect plateau-like surfaces, consistent with less abrasive dietary regimes (Fig. 2A). The substantially reduced  $Smr$  and increased  $Smc$  in later populations indicate deeper surface wear patterns from habitual consumption of abrasive-contaminated foods, likely grit from milling stones<sup>64</sup>.

Considerable intra-period variability was noted within the Pre-Pottery Neolithic and Chalcolithic periods. Within the PPN, differences between the PPNB and PPNC indicate nuanced shifts in dietary practices or local resource utilization (Fig. 3D). The chronological separation along PC1 implies a progressive shift in microwear textures from the middle (PPNB) to late (PPNC) Pre-Pottery Neolithic, with PPNC individuals exhibiting greater heterogeneity ( $Hasfc$ ) yet fewer small peaks, perhaps reflecting changes in food processing or resource availability that reduced fine abrasive loads while increasing overall textural variability (Fig. 3D). The site-level pattern on PC2 suggests that, within each sub-period, local subsistence practices modulated microwear signatures. Atlit-Yam and Abu Gosh share high  $Smr$ , consistent with diets dominated by relatively flat plateau-producing fine abrasives. Conversely, Motza and Kfar HaHoresh exhibit higher  $Smfc$ , pointing to coarser abrasives or tougher food items that generate rougher surfaces with fewer plateaus, possibly linked to inland hunting or less-processed plant resources (Fig. 3D). Higher complexity and peak density observed in the PPNB likely correspond to intensive cereal processing, whereas higher heterogeneity in the PPNC suggests a broader dietary spectrum.

The Chalcolithic period demonstrated notable dietary distinctions among sites, reflecting localized practices (Fig. 3E). The PCA of Chalcolithic sites carried out on six key surface-texture parameters ( $Asfc$ ,  $Spd$ ,  $Sa$ ,  $Smr$ ,  $Smfc$ , and  $Hasfc$ ) reveals site-specific microwear signatures (Fig. 3E). Motza displays very high  $Asfc$ ,  $Smr$ , and  $Spd$  coupled with low  $Hasfc$ , a combination most consistent with intensive fine-particle abrasion, possibly from mineral grit introduced during plant processing. Safsuf, in contrast, is characterised by elevated  $Sa$ , and  $Smfc$ ,

pointing to broad, deep relief features compatible with mastication of harder or more fibrous items, while Asawir shares Safsuf's high *Smfc* yet exhibits the greatest *Hasfc*, suggesting a more variable mechanical regime that may alternate between abrasive and softer diets. Nahal Soreq shows low *Sa*, *Smfc*, and *Spd* combined with high *Hasfc*, a pattern implying predominantly smooth wear surfaces intermittently marked by diverse features, as might arise from a largely soft diet occasionally punctuated by harder particles. Peqi'in occupies an intermediate position for all variables, indicating a balanced wear regime lacking extremes of abrasion or heterogeneity (Fig. 3E). Taken together, these observations point to heterogeneous food-processing techniques and consumption practices across Chalcolithic communities; however, the behavioural scenarios inferred here remain provisional and will require corroboration from complementary archaeological evidence such as botanical, faunal and isotopic data.

The inherent variability in individual wear patterns further complicates interpretations, as observed differences might result from individual dietary habits rather than reflecting broader population trends. Moreover, improper examination can lead to misinterpretation of microwear features. Certain micro-topographical characteristics may be mistakenly attributed to diet when they are actually artifacts resulting from the impression materials used during analysis. The conclusions from the findings should be interpreted carefully, considering these inherent limitations.

This research enhances understanding of dietary evolution in the Levant, highlighting that subtle microwear variations are indicative of dietary shifts and food-processing innovations. Even within each period, subtle differences point to diverse local food practices. By combining Scale-Sensitive Fractal Analysis (SSFA) with 3D surface texture standards (3DST), clear dietary distinctions between Natufian hunter-gatherers and subsequent Pre-Pottery Neolithic and Chalcolithic agriculturalists were effectively captured. The Natufians exhibited dental wear indicative of smoother surfaces and directional chewing consistent with foraging and minimally processed food consumption. In contrast, Pre-Pottery Neolithic and Chalcolithic populations demonstrated increasingly abrasive diets associated with intensive cereal processing and the widespread adoption of grinding tools. Notably, intra-period variations highlighted diverse local dietary practices within these broader subsistence transitions. Although limited by small sample sizes, the findings underscore the utility of integrated DMTA methodologies in reconstructing subtle dietary shifts, emphasizing the need for complementary archaeological evidence to enhance the contextual interpretation of prehistoric subsistence strategies.

## Methods

### Study sample

We analyzed second molars from 78 individuals across 11 archaeological sites in the Levant. All the specimens utilized in the study are housed in the Dan David Center for Human Evolution and Biohistory Research, the Gray Faculty of Medical & Health Sciences, Tel Aviv University, Israel. The sample comprised: 19 Natufian individuals (14,900–11,750 cal BP) from Hayonim and Eynan-Mallaha; 21 Pre-Pottery Neolithic individuals (9,400–7,500 cal BP), including 6 Pre-Pottery Neolithic B (PPNB; 9,400–8,100 BP) from Kfar HaHoresh and Abu Ghosh, and 15 Pre-Pottery Neolithic C (PPNC; 8,100–7,500 BP) from Atlit-Yam and Motza; 19 Chalcolithic individuals (6,500–5,500 cal BP) from Peqi'in, Safsuf, Asawir, Nahal-Soreq, and Motza; Recent modern sample comprised 19 Bedouin individuals from Lahav-Z.

### Dental microwear texture analysis (DMTA)

DMTA targeted facet 9 of mandibular second molars (Fig. 1), selected for its role in Phase II of the chewing cycle<sup>51</sup>. First molars were excluded due to extensive wear, and third molars due to variable morphology and occasional absence (congenital).

The protocol for surface texture analysis was conducted as follows (Fig. 1):

1. **Cleaning:** Contaminants were removed from the dental surfaces using 95% ethanol and cotton wool. An impression material was employed to clear dust from fissures.
2. **Molding:** Obtaining scans directly from the mandibles is technically challenging, since homologous placement of the specimens on the stage of the measuring system is not possible for large specimens. Moreover, the occlusal facets across populations display different reflectivity, which can introduce optical artifacts if scanned directly. High resolution silicone dental impression material (Provil Novo Light CD 2, Heraeus Kulzer GmbH, Dormagen, Germany) was used to mold facets, marked with two colors to indicate the distal and buccal orientations. Following Schulz et al., we avoided producing epoxy resin casts, as each additional replication step risks subtle loss of surface detail<sup>44</sup>.
3. **Surface Measurements:** Measurements were taken directly from the mold immediately after the polymerization of the impression material using a high-resolution confocal disc-scanning measuring system ( $\mu$ surf explorer, NanoFocus AG, Oberhausen, Germany) with a 100 $\times$  long-distance lens and 10 $\times$  internal magnification (total magnification of 1000 $\times$ ) with a 160 $\times$ 160  $\mu$ m field of view. By scanning directly from the silicone impressions we ensured minimal transformation of the original topography. Two to four measurements per facet were collected to provide a representative image of facet 9.

### Data analysis

The resulting 3D surface models were analyzed using two methods via the Mountains Map Premium software (v. 7.3.7; DigitalSurf):

4. **Scale-Sensitive Fractal Analysis (SSFA):** Utilizing SFrax and Toothfrax software packages (Surfract, [www.surfract.com](http://www.surfract.com)) based on Scott et al.<sup>53,57</sup>. The parameters used were complexity (*Asfc*), anisotropy (*epLsar*).
5. **3D Areal Surface Texture Standards (3DST):** Parameters were generated using  $\mu$ soft analysis premium v. 5.0 software (NanoFocus AG, Oberhausen, Germany), a derivative of Mountains Analysis software by Digital

Surf, Besançon, France. ISO/DIS 25178 parameters included: (1) standardized height, (2) spatial, (3) hybrid, (4) functional, and (5) segmentation (Table 1).

### Statistical analysis

Statistical analyses were performed using SPSS (v. 21.0), with significance set at  $p < 0.05$ . Normality was tested with the Kolmogorov-Smirnov test. To compare several groups, normally distributed data were analyzed with One-way ANOVA followed by post hoc Tukey tests; non-normally distributed data were analyzed with the Kruskal-Wallis test followed by multiple comparisons with Bonferroni adjustments. To compare two groups (intra-period comparison: PPNB vs PPNC) - variables that were found to be normally distributed were analyzed using an independent sample T-test, while non-normal distributed variables were analyzed using the Mann-Whitney U test. PCA was conducted using PAST software (v. 5.0.2;<sup>68</sup>) to visualize variance in microwear parameters.

### Data availability

The datasets used and/or analyzed during the current study available from the corresponding author on reasonable request.

Received: 2 July 2025; Accepted: 24 November 2025

Published online: 09 December 2025

### References

1. Hershkovitz, I. & Gopher, A. Demographic, biological and cultural aspects of the neolithic revolution: A view from the southern Levant. In Bocquet-Apple, J. P. & Bar-Yosef, O. (eds.) *The Neolithic demographic transition and its consequences*, The Neolithic Demographic Transition and its Consequences, 441–479 (Springer, 2008).
2. Kuijt, I. & Goring-Morris, N. Foraging, farming, and social complexity in the Pre-Pottery Neolithic of the southern Levant: A review and synthesis. *Journal of World Prehistory* **16**, 361–440 (2002).
3. Kuijt, I. & Finlayson, B. Evidence for food storage and predomestication granaries 11,000 years ago in the Jordan Valley. *Proc Natl Acad Sci USA* **106**, 10966–10970 (2009).
4. Goring-Morris, A. N. & Belfer-Cohen, A. Neolithization processes in the Levant: The outer envelope. *Current Anthropology* **52**, S195–S208 (2011).
5. Lieberman, D. E. Seasonality and gazelle hunting at Hayonim Cave: New evidence for sedentism during the Natufian. *Paleorient* 47–57 (1991).
6. Bar-Yosef, O. From sedentary foragers to village hierarchies: the emergence of social institutions. In *Proceedings of the British Academy*, vol. 110, 1–38 (Oxford University Press, 2001).
7. Belfer-Cohen, A. & Goring-Morris, A. N. Becoming farmers: The inside story. *Current Anthropology* **52**, S209–S220 (2011).
8. Smith, P., Bloom, R. A. & Berkowitz, J. Diachronic trends in humeral cortical thickness of Near Eastern populations. *Journal of human evolution* **13**, 603–611 (1984).
9. Smith, P., Bar-Yosef, O. & Sillen, A. Archaeological and skeletal evidence for dietary change during the late Pleistocene/Early Holocene in the Levant. *Paleopathology at the Origins of Agriculture* 101–136 (1984).
10. Bar-Yosef, O. & Belfer-Cohen, A. The origins of sedentism and farming communities in the Levant. *Journal of World Prehistory* **3**, 447–498 (1989).
11. Yeshurun, R., Bar-Oz, G. & Weinstein-Evron, M. Modern hunting behavior in the early Middle Paleolithic: Faunal remains from Misliya Cave, Mount Carmel. *Israel. Journal of human evolution* **53**, 656–677 (2007).
12. Nadel, D., Rosenberg, D. & Yeshurun, R. The deep and the shallow: The role of Natufian bedrock features at Rosh Zin, Central Negev, Israel. *Bulletin of the American Schools of Oriental Research* 1–29 (2009).
13. Valla, F. R., Khalaily, H., Samuelian, N. & Bocquentin, F. From foraging to farming. The contribution of the Mallaha (Eynan) excavations, 1996–2001. *Bulletin du Centre de recherche français à Jérusalem* 71–90 (2002).
14. Yeshurun, R., Bar-Oz, G. & Weinstein-Evron, M. Intensification and sedentism in the terminal Pleistocene Natufian sequence of el-Wad Terrace (Israel). *Journal of human evolution* **70**, 16–35 (2014).
15. Nadel, D. & Lengyel, G. Human-made bedrock holes (mortars and cupmarks) as a Late Natufian social phenomenon. *Archaeology, Ethnology and Anthropology of Eurasia* **37**, 37–48 (2009).
16. Horwitz, L. K. *et al.* Animal domestication in the southern Levant. *Paleorient* 63–80 (1999).
17. Willcox, G. The distribution, natural habitats and availability of wild cereals in relation to their domestication in the Near East: Multiple events, multiple centres. *Vegetation History and Archaeobotany* **14**, 534–541 (2005).
18. Zeder, M. A. The origins of agriculture in the Near East. *Current Anthropology* **52**, S221–S235 (2011).
19. Bar-Yosef, O. The Natufian culture in the Levant, threshold to the origins of agriculture. *Evolutionary Anthropology: Issues, News, and Reviews: Issues, News, and Reviews* **6**, 159–177 (1998).
20. Finlayson, B. *et al.* Architecture, sedentism, and social complexity at Pre-Pottery Neolithic A WF16, Southern Jordan. *Proceedings of the National Academy of Sciences* **108**, 8183–8188 (2011).
21. Kislev, M. E. Emergence of wheat agriculture. *Paleorient* **10**, 61–70 (1984).
22. Garfinkel, Y., Kislev, M. E. & Zohary, D. Lentil in the Pre-Pottery Neolithic B Yiftahel: Additional evidence of its early domestication. *Israel journal of botany* (1988).
23. Verhoeven, M. Beyond boundaries: Nature, culture and a holistic approach to domestication in the Levant. *Journal of World Prehistory* **18**, 179–282 (2004).
24. Peters, J., von den Driesch, A., Helmer, D. & Segui, M. S. Early animal husbandry in the Northern Levant. *Paleorient* 27–48 (1999).
25. Garfinkel, Y. Burnt lime products and social implications in the Pre-Pottery Neolithic B villages of the Near East. *Paleorient* 69–76 (1987).
26. Khalaily, H. *et al.* Excavations at Motza in the Judean Hills and the early Pre-Pottery Neolithic B in the southern Levant. *Paleorient* 5–37 (2007).
27. Khalaily, H. *et al.* Recent excavations at the Neolithic site of Yiftahel (Khalet Khalladyah), lower Galilee. *Neo-lithics* **2**, 3–11 (2008).
28. Gopher, A. Horvat Galil—an early PPNB site in the Upper Galilee. *Israel. Tel Aviv* **1997**, 183–222 (1997).
29. Molleson, T. Bones of work at the origins of labour. *Archaeology and Women: Ancient and Modern Issues*. S. Hamilton, RD Whitehouse, and KI Wright, eds 185–198 (2007).
30. Galili, E. *et al.* Atlit-Yam: A prehistoric site on the sea floor off the Israeli coast. *Journal of Field Archaeology* **20**, 133–157 (1993).
31. Galili, E., Lernau, O. & Zohar, I. Fishing and Coastal Adaptations at Atlit-Yam —A Submerged PPNC Fishing Village off the Carmel Coast. *Israel. Atiqot* **48**, 1–34 (2004).

32. Evershed, R. P. et al. Earliest date for milk use in the Near East and southeastern Europe linked to cattle herding. *Nature* **455**, 528–531 (2008).
33. Gilead, I. The chalcolithic period in the Levant. *Journal of World Prehistory* **2**, 397–443 (1988).
34. Rowan, Y. M. & Golden, J. The Chalcolithic period of the Southern Levant: A synthetic review. *Journal of World Prehistory* **22**, 1–92 (2009).
35. Eshed, V., Gopher, A., Galili, E. & Hershkovitz, I. Musculoskeletal stress markers in Natufian hunter-gatherers and Neolithic farmers in the Levant: The upper limb. *American Journal of Physical Anthropology* **123**, 303–315 (2004).
36. Eshed, V., Gopher, A. & Hershkovitz, I. Tooth wear and dental pathology at the advent of agriculture: new evidence from the Levant. *American Journal of Physical Anthropology* **130**, 145–159 (2006).
37. Eshed, V., Gopher, A., Pinhasi, R. & Hershkovitz, I. Paleopathology and the origin of agriculture in the Levant. *American Journal of Physical Anthropology* **143**, 121–133 (2010).
38. Smith, P. Diet and attrition in the Natufians. *American Journal of Physical Anthropology* **37**, 233–238 (1972).
39. Smith, B. H. Patterns of molar wear in hunter-gatherers and agriculturalists. *American Journal of Physical Anthropology* **63**, 39–56 (1984).
40. Walker, P. L. A quantitative analysis of dental attrition rates in the Santa Barbara Channel area. *American Journal of Physical Anthropology* **48**, 101–106 (1978).
41. Mahoney, P. Dental microwear from Natufian hunter-gatherers and early Neolithic farmers: Comparisons within and between samples. *American journal of physical anthropology* **130**, 308–319 (2006).
42. Schmidt, C. W. et al. Dental microwear texture analysis of Homo sapiens sapiens: Foragers, farmers, and pastoralists. *American journal of physical anthropology* **169**, 207–226 (2019).
43. El Zaatri, S. Occlusal microwear texture analysis and the diets of historical/prehistoric hunter-gatherers. *International Journal of Osteoarchaeology* **20**, 67–87 (2010).
44. Schulz, E., Calandra, I. & Kaiser, T. M. Applying tribology to teeth of hoofed mammals. *Scanning* **32**, 162–182 (2010).
45. El Zaatri, S. & Hublin, J. Diet of Upper Paleolithic modern humans: Evidence from microwear texture analysis. *American journal of physical anthropology* **153**, 570–581 (2014).
46. El Zaatri, S., Grine, F. E., Ungar, P. S. & Hublin, J. J. Ecogeographic variation in Neandertal dietary habits: Evidence from occlusal molar microwear texture analysis. *Journal of Human Evolution* **61**, 411–424 (2011).
47. Schmidt, C. W., Beach, J. J., McKinley, J. I. & Eng, J. T. Distinguishing dietary indicators of pastoralists and agriculturists via dental microwear texture analysis. *Surface Topography: Metrology and Properties* **4**, 14008 (2015).
48. Schmidt, C. W., El Zaatri, S. & Van Sessen, R. Dental microwear texture analysis in bioarchaeology. In *Dental Wear in Evolutionary and Biocultural Contexts*, 143–168 (Elsevier, 2020).
49. Hernando, R. et al. What about the buccal surfaces? dental microwear texture analysis of buccal and occlusal surfaces refines paleodietary reconstructions. *American Journal of Biological Anthropology* **178**, 347–359 (2022).
50. Sarig, R. et al. How did the qesem cave people use their teeth? analysis of dental wear patterns. *Quaternary International* **398**, 136–147 (2016).
51. Kay, R. F. & Hiiemae, K. M. Jaw movement and tooth use in recent and fossil primates. *American Journal of Physical Anthropology* **40**, 227–256 (1974).
52. Krueger, K. L., Scott, J. R., Kay, R. F. & Ungar, P. S. Technical note: Dental microwear textures of Phase I and Phase II facets. *American Journal of Physical Anthropology* **137**, 485–490 (2008).
53. Scott, R. S. et al. Dental microwear texture analysis: technical considerations. *Journal of Human Evolution* **51**, 339–349 (2006).
54. Boyde, A. & Jones, S. J. Mapping and measuring surfaces using reflection confocal microscopy. In *Handbook of Biological Confocal Microscopy*, 255–266 (Springer, 1995).
55. Ungar, P. S., Brown, C. A., Bergstrom, T. S. & Walker, A. Quantification of dental microwear by tandem scanning confocal microscopy and scale-sensitive fractal analyses. *Scanning* **25**, 185–193 (2003).
56. Scott, R. Dental microwear texture analysis reflects diets of living primates and fossil hominins. *Nature* **436**, 693–695 (2005).
57. Scott, R. S. et al. Dental microwear texture analysis shows within-species diet variability in fossil hominins. *Nature* **436**, 693–695 (2005).
58. Specifications, G. P. Surface texture: Areal—part 2: Terms, definitions and surface texture parameters. *International Organization for Standardization* **25178–2** (2012).
59. Kaiser, T. M. & Brinkmann, G. Measuring dental wear equilibria—the use of industrial surface texture parameters to infer the diets of fossil mammals. *Palaeogeography, Palaeoclimatology, Palaeoecology* **239**, 221–240 (2006).
60. Power, R. C. & Williams, F. L. Evidence of increasing intensity of food processing during the upper paleolithic of western eurasia. *Journal of Paleolithic Archaeology* **1**, 281–301 (2018).
61. Williams, F., Schmidt, C. & Droke, J. Inferring the diet of late neolithic hastière caverne m from the meuse basin of belgium. *Anthropologica et Préhistorica* **131**, 79–96 (2022).
62. Bar-Yosef, O. & Meadow, R. H. The origins of agriculture in the Near East. In *Last hunters, first farmers: New perspectives on the prehistoric transition to agriculture*, 39–94 (School of American Research Press (eds Price, T. & Gebauer, A.) (Santa Fe, New Mexico, 1995).
63. Hopf, M. & Bar-Yosef, O. Plant remains from hayonim cave, western galilee. *Paleorient* **117**–120 (1987).
64. Wright, K. I. Ground-stone tools and hunter-gatherer subsistence in southwest Asia: Implications for the transition to farming. *American Antiquity* **59**, 238–263 (1994).
65. Baker, G., Jones, L. & Wardrop, I. Cause of wear in sheep's teeth. *Nature* **184**, 1583–1584 (1959).
66. Pough, F. H. *A field guide to rocks and minerals* (Houghton Mifflin Harcourt, 1996).
67. Pastor, R. F. *Dental microwear among prehistoric inhabitants of the Indian subcontinent: a quantitative and comparative analysis* (University of Oregon, 1993).
68. Hammer, O. & Harper, D. A. T. Past: Paleontological statistics software package for education and data analysis. *Palaeontologia electronica* **4**, 1 (2001).

## Acknowledgements

This research was supported by the Israel Science Foundation (ISF), grants No. 632/20 and 654/20 to D.Z.B., grant No. 1005/22 to H.M., and grant No. 1339/19 to R.S. We gratefully acknowledge the archaeologists Ofer Bar-Yosef, Liliane Meignen, François Valla, Hamudi Khalaily, Nigel Goring-Morris, Ehud Galili, Jacob Vardi, Dina Shalem, Ianir Milevski, Lena Brailovsky-Rokser and Ofer Marder, together with the anthropologists Israel Hershkovitz, Fanny Bocquentin, Marie Anton, and Yossi Nagar, whose devoted fieldwork at the excavation sites laid the indispensable foundations for this study.

## Author contributions

D.M.: conceptualization, investigation, data curation, writing—original draft; A.P.: conceptualization, formal analysis, visualization, writing – original draft; H.M.: resources, methodology, writing – review & editing;

D.Z.B.: validation, methodology, writing – review & editing; R.S.: conceptualization, investigation, supervision, project administration, funding acquisition, writing – review & editing. All authors reviewed and approved the final manuscript.

## Declarations

### Competing interests

The authors declare no competing interests.

### Additional information

**Correspondence** and requests for materials should be addressed to R.S.

**Reprints and permissions information** is available at [www.nature.com/reprints](http://www.nature.com/reprints).

**Publisher's note** Springer Nature remains neutral with regard to jurisdictional claims in published maps and institutional affiliations.

**Open Access** This article is licensed under a Creative Commons Attribution-NonCommercial-NoDerivatives 4.0 International License, which permits any non-commercial use, sharing, distribution and reproduction in any medium or format, as long as you give appropriate credit to the original author(s) and the source, provide a link to the Creative Commons licence, and indicate if you modified the licensed material. You do not have permission under this licence to share adapted material derived from this article or parts of it. The images or other third party material in this article are included in the article's Creative Commons licence, unless indicated otherwise in a credit line to the material. If material is not included in the article's Creative Commons licence and your intended use is not permitted by statutory regulation or exceeds the permitted use, you will need to obtain permission directly from the copyright holder. To view a copy of this licence, visit <http://creativecommons.org/licenses/by-nc-nd/4.0/>.

© The Author(s) 2025